Neural Comput & Applic (2014) 24:1079–1087
DOI 10.1007/s00521-012-1333-3

ORIGINAL ARTICLE

Prediction of suspended sediment concentration from water quality variables

Adem Bayram · Murat Kankal · Gökmen Tayfur · Hızır Önsoy

Received: 8 June 2012 / Accepted: 29 December 2012 / Published online: 11 January 2013

Abstract This study investigates use of water quality (WQ) variables, namely total chromium concentration, total iron concentration, and turbidity for predicting suspended sediment concentration (SSC). For this purpose, the artificial neural networks (ANNs) and regression analysis (RA) models are employed. Seven different RA models are constructed, considering the functional relation between measured WQ variables and SSC. The WQ and SSC data are fortnightly obtained from six monitoring stations, located on the stream Harsit, Eastern Black Sea Basin, Turkey. A total of 132 water samples are collected from April 2009 to February 2010. Model prediction results reveal that ANN is able to predict SSC from WQ data, with mean absolute error (MAE) of 10.30 mg/L and root mean square error (RMSE) of 13.06 mg/L. Among seven RA models, the best one, which has the form including all independent parameters, produces results comparable to those of ANN, with MAE = 14.28 mg/L and RMSE = 15.35 mg/L. The sensitivity analysis results reveal that the most effective parameter on the SSC is total chromium concentration. These results have time- and cost-saving implications.

Keywords Artificial neural networks · Regression analysis · Stream Harsit · Suspended sediment concentration · Total chromium · Total iron · Turbidity

A. Bayram (✉) · M. Kankal · H. Önsoy
Department of Civil Engineering, Faculty of Engineering, Karadeniz Technical University, 61080 Trabzon, Turkey
e-mail: adembayram@gmail.com

G. Tayfur
Department of Civil Engineering, Faculty of Engineering, Izmir Institute of Technology, 35340 Izmir, Turkey

1 Introduction

Suspended sediment is a constituent of water quality (WQ) that is monitored because of concerns about accelerated erosion, nonpoint contamination of water resources, and degradation of aquatic environments [1]. The transport of sediment in rivers is also important with respect to channel navigability, reservoir filling, hydroelectric-equipment longevity, fish habitat, river esthetics, and other scientific interests [2]. Sediment loads in rivers basically consist of bed load and suspended sediment [3]. Suspended sediment constitutes 75–95 % of the total load [4].

Suspended sediment load (SSL) of a river is generally obtained by direct analysis of the SSC or by using sediment-rating curve (SRC) method. Although direct analysis is the most dependable method, it is very costly, time consuming, and, in many instances, problematic for inaccessible sections, especially during floods, and cannot be conducted for all river gauge stations. This may be the reason for having fewer operational sediment gauging stations on Turkish rivers. In general, before building a water structure such as a dam or a weir, the EİE (General Directorate of Electrical Power Resources Survey and Development Administration) or the DSİ (General Directorate of State Hydraulic Works) builds temporary gauging stations to measure sediment. Soon after the structure becomes operational, the gauging stations are either removed or not operated [5–8]. Hence, researchers have looked for alternative options for sediment predictions. One of these options is to do the predictions using other parameters, such as discharge [9], precipitation [3], turbidity [1, 10], and water quality [11].

Much research has been done to correlate secondary parameters to suspended sediment, such as discharge, turbidity, and water density. Minella et al. [10] assessed the relationship between SSC and turbidity for a small

(1.19 km^2) rural catchment in southern Brazil, and evaluated two calibration methods by comparing the estimates of SSC obtained from the calibrated turbidity readings with direct measurements obtained using a suspended sediment sampler. Meral et al. [11] used two practical and relatively cheap alternative methods (namely turbidity sensor and Imhoff cone method) to estimate SSC. Williamson and Crawford [1] aimed to quantify the potential for estimating SSC using two surrogate sediment parameters (TSS and turbidity) in order to enable regional and site-specific modeling of sediment concentrations in Kentucky streams.

Recently, the neural networks approach has been applied to many branches of science [12–16]. The approach is becoming a strong tool for providing hydraulic and environmental engineers with sufficient details for design purposes and management practices. The technique has a growing body of applications for river engineering and water resources [17–19]. ANNs employment in suspended sediment estimation and prediction has been worked out. Nagy et al. [9] developed an ANN model to estimate SSC in rivers, achieved by training the ANN model to extrapolate several stream data collected from reliable sources. The network was set up using several parameters, such as Froude number, stream width ratio, mobility number and Reynolds number, as the input pattern and the SSC as the output pattern. Kisi et al. [20] analyzed and discussed the performance of adaptive neuro-fuzzy technique, radial basis neural network, feed-forward neural network, and generalized regression neural network in the prediction of suspended sediment. Rajaee et al. [21] considered ANNs, neuro-fuzzy, multi-linear regression, and conventional SRC models for time series modeling of SSC in rivers. The models are trained using daily river discharge and SSC data belonging to Little Black River and Salt River gauging stations in the USA. Wang et al. [22] investigated the potential of two algorithm networks, the feed-forward back propagation and generalized regression neural network, in comparison with the classical regression for modeling the event-based SSC at Jiasian diversion weir in Southern Taiwan. Mount and Abrahart [23] reported a comprehensive set of single-input single-output neural network suspended sediment modeling experiments performed on two catchments in Puerto Rico. Bayram et al. [24] evaluated whether the turbidity can produce a satisfactory prediction of the SSC, and improve an ANN method estimating the SSC based on in situ turbidity measurements in the stream Harsit, Eastern Black Sea Basin, Turkey. Demirci and Baltaci [25] proposed a fuzzy logic approach to estimate SSC from streamflow.

The stream Harsit having a length of 143 km and catchment area of 3,280 km^2 is an important sub-watershed in the Eastern Black Sea Basin, Turkey. There are two large dams and a lot of hydroelectric power plants (HEPPs) on the Harsit. The watershed is susceptible to erosion due to its vegetation cover and steep topography. For example, SSC values can exceed 500 mg/L for the upstream of Torul Dam in operation on the stream Harsit. There are a number of flow monitoring stations operated by DSİ and EİE on the watershed, but SSC monitoring is not sufficient. Therefore, determination of SSC values along the stream Harsit is very important with respect to life and management of the water structures.

The purpose of this paper is to investigate whether WQ variables of total chromium concentration (mg Cr/L), total iron concentration (mg Fe/L), and turbidity (NTU) can produce a sufficient prediction of the SSC. Cr and Fe concentrations are used for the first time to predict the SSC. A surface water quality study including twenty variables was conducted on a fortnightly basis from April 2009 to February 2010 for the stream Harsit. Of these variables, by the factor analysis, only three were selected as model input vectors.

2 Artificial neural network approach

ANNs are inspired by biological systems with large numbers of neurons, which collectively perform tasks that even the largest computers have been unable to match. The function of an artificial neuron is similar to that of a real neuron: It communicates by sending signals to other artificial neurons over a large number of biased or weighted connections. Each of these neurons has an associated transfer function describing how the weighted sum of its input is converted to an output (Fig. 1).

There are different types of ANNs, based on neuron arrangement and their connections, and training paradigm. Among the various types of ANNs, the multi-linear perceptron (MLP) network trained with the back propagation algorithm is the most common one in engineering applications [26].

In a feed-forward ANN, the input quantities are fed into the input layer neurons that, in turn, pass them on to the hidden layer neurons after multiplication by connection weights. A hidden layer neuron adds up the weighted input received from each input neuron and associates it with a

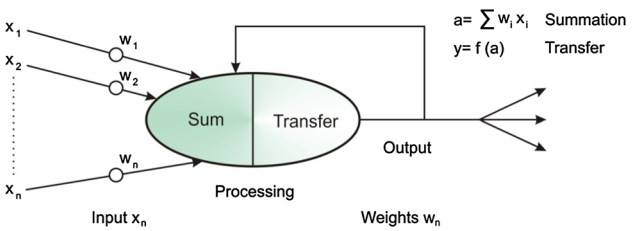

Fig. 1 Artificial neuron

bias. The result is then passed on through a nonlinear transfer function to produce an output.

The learning of ANNs is generally accomplished by the most commonly used supervised training algorithm of the back propagation algorithm. The objective of this algorithm is to find the optimal weights that would generate an output vector $\boldsymbol{Y} = (y_1, y_2, \ldots, y_p)$ as close as possible to the target values of the output vector $\boldsymbol{T} = (t_1, t_2, \ldots, t_p)$ with the selected accuracy. The optimal weights are found by minimizing a predetermined error function (E) of the following form [26]:

$$E = \sum_{P} \sum_{p} (y_i - t_i)^2 \quad (1)$$

where y_i = the component of an ANN output vector $\boldsymbol{Y}$; t_i = the component of a target output vector $\boldsymbol{T}$; p = the number of output neurons; and P = the number of training patterns.

In the back propagation algorithm, the effect of the input is first passed forward through the network to reach the output layer. After the error is computed, it is then propagated back toward the input layer with the weights being modified. The gradient-descent method, along with the chain rule of differentiation, is employed to modify the network weights as [26]:

$$\Delta v_{ij}(n) = -\delta \frac{\partial E}{\partial v_{ij}} + \alpha \Delta v_{ij}(n-1) \quad (2)$$

where $\Delta v_{ij}(n)$ and $\Delta v_{ij}(n-1)$ = the weight increments between node i and j during the nth and $(n-1)$th pass or epoch; δ = the learning rate; and α = the momentum factor.

Figure 2 schematically presents the MLP employed in this study. The details of ANNs are given in Tayfur [26].

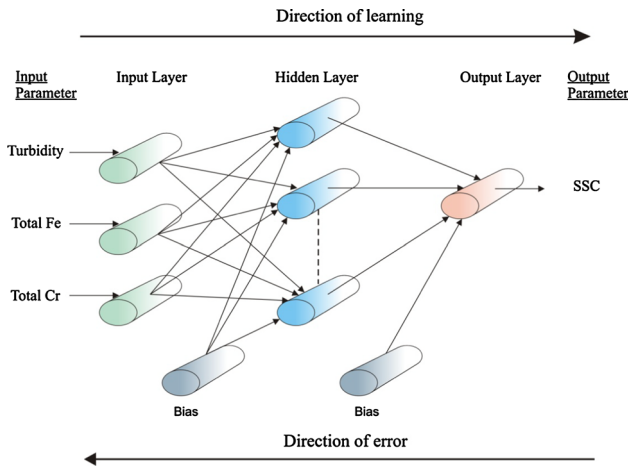

Fig. 2 The architecture of back propagation network model

3 The study area

Turkey is hydrologically divided into 26 drainage basins. Eastern Black Sea Basin having a recharge area of 24,077 km^2 and a surface water potential of 15,331 billion cubic meters is one of the most important basins in Turkey and a major part of Caucasus Ecological Region together with Coruh and Aras Basins (Fig. 3). The Eastern Black Sea Basin consists of 17 sub-watersheds, and the stream Harsit watershed having a main branch length of 143 km, and catchment area of 3,280 km^2 has a place in these sub-watersheds [24, 27–32].

The stream Harsit originates from Vauk Mountains in the east border of Gumushane Province and formed by small streams joining together. After it is formed, Harsit passes through the towns and cities, namely Tekke, Gumushane, Torul, Ozkurtun, Kurtun, and Dogankent, respectively, and poured into the Black Sea in Tirebolu town of Giresun Province (Fig. 3). The streams Arzular, Korum, Ikisu, Cit, Kurtun, and Gavraz are important tributaries of it. There are four HEPPs in operation for the time being on Harsit, namely Akkoy I HEPP, Dogankent HEPP, Kurtun Dam and HEPP, Torul Dam and HEPP [24, 27–32]. Many dams and HEEPs are also under construction or planned, namely Akkoy II, Aladerecam, Aslancik, Avluca, Cileklikaya, Duzoren, Elmali, Gocen, Gokcebel, Koru, Kovacik, Kuletas, Tasoba, Tirebolu, Sogukpinar, Yasmakli, and so on.

4 Materials and methods

4.1 Turbidity measurements

The stream water turbidity was determined in situ using portable field meter in terms of nephelometric turbidity units (NTU). The field meter uses the light-absorption–scattering method. Irradiation of a beam of light onto a sample brings about separation of the beam into (1) the light transmitted by the solution and (2) the light scattered by turbidity components in the sample. In the light-absorption–scattering method, the intensity of both transmitted light and the scattered light are measured using separate receptors, and the turbidity is obtained based on the ratio of the two.

4.2 Surface water sampling

The surface water samples were fortnightly hand-collected at six monitoring stations named as H1, H2, H3, H4, H5, and H6, which are located in the course of the stream Harsit before the Torul concrete faced rock-fill dam during the study period of April 2009–February 2010 (Fig. 3). Detailed information of the sampling points is given in Table 1. One-liter surface water was sampled from

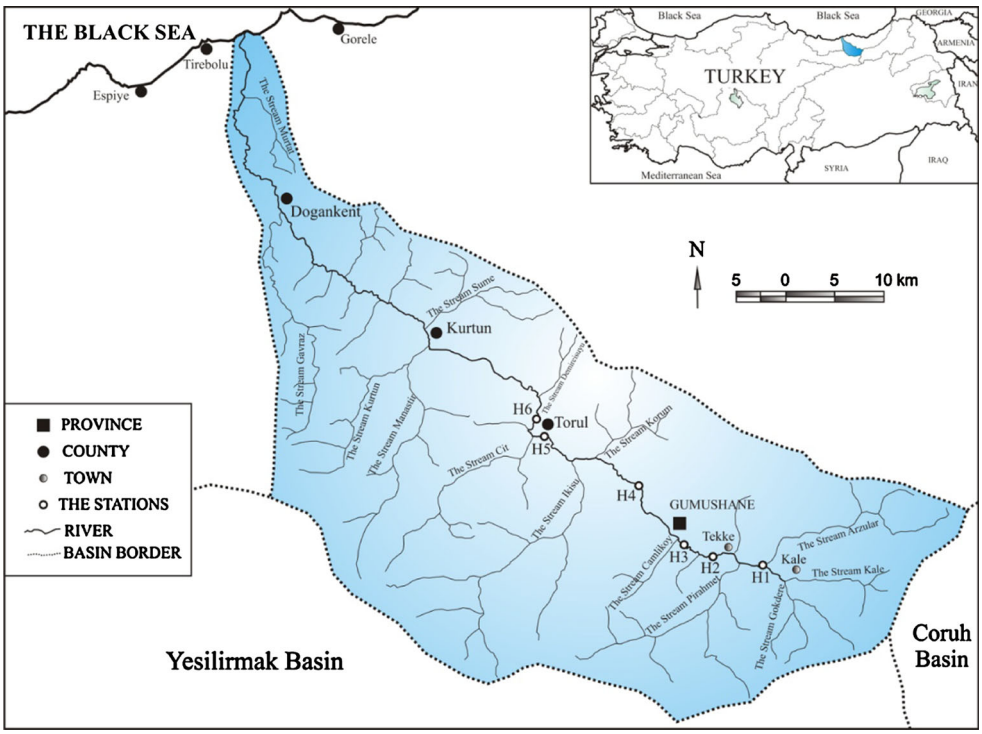

Fig. 3 Locations of study area and sampling sites on the stream Harsit

Table 1 Localization of the surface water sampling stations in the stream Harsit

The stations	Coordinates	Altitude (m)	km of the course
H1	40°24′07.4″N–39°38′29.3″E	1,274	0.0
H2	40°24′54.0″N–39°34′37.6″E	1,234	6.5
H3	40°25′23.6″N–39°31′37.7″E	1,190	12.5
H4	40°29′36.6″N–39°27′30.4″E	1,100	24.0
H5	40°32′55.7″N–39°18′52.5″E	939	39.5
H6	40°33′56.7″N–39°17′54.6″E	910	45.0

approximately mid-depth of flow. High-density polyethylene bottles having 500 mL volume were rinsed with the stream water, shaken vigorously, and emptied before refilling for the analysis [24, 33]. Sampling, preservation, and transportation of the stream water samples to the laboratory were as per standard methods [34].

4.3 Determination of the SSC

The surface water samples were firstly filtered through a glass microfiber disc (Sartorius, FT-3-1103-055) having 1.2-μm pore size under vacuum in order to separate the water from the suspended sediment; once the water was clarified, the material collected was then oven-dried at 105 °C for about 12 h, until the matter reached a constant weight. SSC was then determined in laboratory in terms of mg/L [24, 33].

4.4 Determination of the total chromium and total iron

Total chromium and total iron concentrations from sediment and water for the unfiltered surface water samples were determined using a UV–vis spectrophotometer according to the standard methods [34]. The analyses were carried out in triplicate in room temperature (21 ± 2 °C) and their mean values were used.

5 SSC prediction

5.1 Regression model

Multiple linear and nonlinear (exponential, power, logarithmic, inverse, joint, growth, and S functions) regression analyses were performed. The following seven models which produced satisfactory results are presented here as follows:

$$\text{Model 1}: \text{SSC} = c + b_1 T + b_2 T^2 + b_3 T^3 \quad (3)$$

$$\text{Model 2}: \text{SSC} = c + b_1 \,\text{Cr} + b_2 \,\text{Cr}^2 + b_3 \,\text{Cr}^3 \quad (4)$$

$$\text{Model 3}: \text{SSC} = c + b_1 \,\text{Fe} + b_2 \,\text{Fe}^2 + b_3 \,\text{Fe}^3 \quad (5)$$

$$\text{Model 4}: \text{SSC} = c\,\text{Cr}^{b_2}\text{Fe}^{b_3} \quad (6)$$

$$\text{Model 5}: \text{SSC} = \exp\left(c + b_1 T + b_2 \,\text{Cr}\right) \quad (7)$$

$$\text{Model 6}: \text{SSC} = \exp\left(c + b_1 T + b_3 \,\text{Fe}\right) \quad (8)$$

$$\text{Model 7}: \text{SSC} = \exp\left(c + b_1 T + b_2 \,\text{Cr} + b_3 \,\text{Fe}\right) \quad (9)$$

Table 2 Regression coefficients and R^2 value for the regression analysis

Model no.	c	b_1	b_2	b_3	R^2
1	15.383	0.036	0.003	-2.263×10^6	0.813
2	1.122	1,053.972	2,743.952	4,721.486	0.789
3	27.098	−16.833	17.016	−1.050	0.824
4	21.417	–	1.384	−0.057	0.804
5	3.423	0.002	–	6.346	0.875
6	3.440	0.001	0.226	–	0.835
7	3.405	0.002	0.042	5.318	0.876

In these equations, b_1, b_2, b_3, and c are the regression coefficients. The regression coefficients were estimated by the least squares method for all of the models. The R^2 values for the models are given in Table 2.

5.2 ANN model

The main objective of this section is to develop an ANN model that predicts the SSC from given total Cr, total Fe, and turbidity data. When designing an ANN, it is important to choose the proper network size. If the network is too small, it may not have enough free parameters to represent the data adequately. If the network is too big, it can either fail to classify the data as meaningful categories or reject new patterns as too dissimilar from the training set. In general, finding a suitable network structure is a matter of trial and error, although an educated guess can be made by comparing the size of the training data set to the number of free parameters in the network. As shown in Fig. 2, a three-layer, feed-forward network is selected for this study. Each layer is fully connected to the next, but no connections exist between neurons in the same layer. The first and third layers contain the input and output variables, respectively. Seven different models were used to train the neural network (Fig. 4). The SSC is the output variable for all models. The order of variables in the input layers is turbidity, total Cr, and total Fe, respectively.

The fortnightly stream WQ data are divided into 96 training, 24 testing, and 12 validation patterns, respectively. Input values for the testing, training, and validation data are shown in Table 3.

Before the training of the network, the data are normalized to range [0.1, 0.9] since the sigmoid activation function is used.

The selected network size represents a compromise between generalization and convergence. Convergence is the capacity of the network to learn the pattern in the training set, and generalization is its capacity to respond correctly to new patterns. One hidden layer is sufficient for most applications [12]. Since determining the number of nodes in the hidden layer is not an exact science, several networks with different numbers of hidden nodes are tested. The parameters of the optimum ANN structures are given in Table 4. To begin the training process, all of the training patterns are introduced a network initialized with random weights.

In this study, the weights are initialized into random values between −0.5 and +0.5, according to commonly accepted procedure. The factors α and δ in Eq. (2) also influence the convergence. The learning rate (δ) is the constant of proportionality for the generalized back propagation rule. The larger its value, the greater the changes in the weights at each iteration. The momentum term (α) is used to prevent the network from oscillating around a local minimum in the parameter space. Several combinations of α and δ are tested in order to find a neural network with good convergence (Table 4).

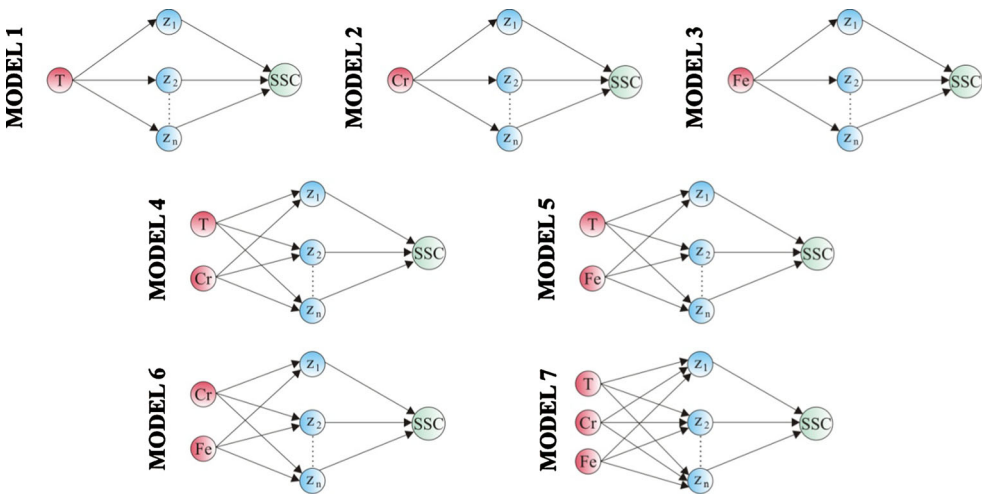

Fig. 4 ANNs architectures used for the prediction of the SSC

Table 3 Fortnightly data used in the ANNs models

The stations	The monitoring and sampling period: April 2009 - February 2010			
	Spring	Summer	Autumn	Winter
H1	▲ x x x ■ x x ▲ x x ■ x x x ▲ x x x x x x ▲			
H2	x ■ x ▲ x x x x x x x x ▲ x ▲ x x x ■ x ▲ x			
H3	x ▲ x x ▲ ■ x x x ▲ x x x x x ■ x x x ▲ x x			
H4	x ▲ x x ■ x x x ▲ x x ■ x x x x x ▲ x x ▲ x			
H5	x x x ▲ x ■ x x ▲ x x x x x x ▲ x x x ■ ▲ x			
H6	x x x x ▲ x x x ▲ x x x x x x ■ x x ▲ ■ x ▲			

x = training set, ▲ = testing set, ■ = validation set

Table 4 Parameters used for different ANN structures

Number of hidden layer unit	Learning rate (α)	Momentum (δ)
2	0.10	0.10
3	0.25	0.25
5	0.50	0.50
8	0.75	0.75
	1.00	1.00

Memorization (overtraining) is a fundamental problem encountered in training of ANN. To prevent this, the training is terminated when the network begins to memorize by using the cross-validation patterns [26]. In this situation, training set error continues to decrease, although testing set error does not change. The performance of a network may be enhanced by increasing the number of training samples, the length of training (number of epochs), or the number of hidden layer nodes. Choosing different values for the learning rate (α) and momentum (δ) may also change the performance of a network. However, all of these methods increase the computation time required to train the network. It is very important to strike a balance between performance and training time. Table 5 shows the structure of the ANNs giving the best results.

6 Results and discussion

When the ANN analysis was performed with the models 1, 2, 3, 4, 5, 6, and 7, the minimum root mean square error (RMSE) in the testing sets was obtained for the model 7 with $\alpha = 1.00$ and $\delta = 0.75$ as 20.38 mg/L (Table 5). The smallest mean absolute error (MAE) of the testing data set in this case was 11.67 mg/L. Errors may be reduced if the stopping criterion, the epoch number, is increased. Besides, conjugate gradient or scaled conjugate gradient methods may be used to reduce maximum relative error instead of generalized delta rule in learning. Also, different network structures with one or more hidden layers or nodes with different learning rates and momentum terms may produce smaller error.

Figures 5 and 6 display the performances of the ANN and regression analyses for the testing and validation data, and the accuracy of the ANN approach for the best-fitting model (model 7). Each plus sign stands for a testing and validation vectors in the both figures. Also, the results obtained from RA for the same values are shown with multiply sign in the same figures. The nearer the points gather around the diagonal, the better the learning results are. The RMSE and MAE of the points on the diagonal are zero. While the RMSE and MAE values obtained from the testing set for the ANNs in the model 7 are 20.38 and 11.67 mg/L, these values for the RA are 29.43 and 21.56 mg/L, respectively. Similarly, the RMSE and MAE for the validation set in the ANNs in the model 7 are 13.05 and 10.29 mg/L, and the same values for the RA are 15.35 and 14.28 mg/L, respectively (Table 6).

7 Sensitivity analysis

Sensitivity analysis was performed to describe the relations between input and output parameters. To that end, cosine amplitude method was selected. This method is one of the

Table 5 Characteristics of ANN giving the best results

Model no	Number of hidden layer unit	α	δ	Epoch	Training error	Testing error
1	3	0.25	1.00	46	0.9219	0.0152
2	3	1.00	0.10	142	0.9053	0.0148
3	2	0.50	0.10	73	0.9735	0.0159
4	5	0.10	1.00	13,901	0.1230	0.0145
5	2	0.10	0.10	32	0.6914	0.0147
6	8	0.10	1.00	11	0.7293	0.0137
7	8	1.00	0.75	20,000	0.1242	0.0128

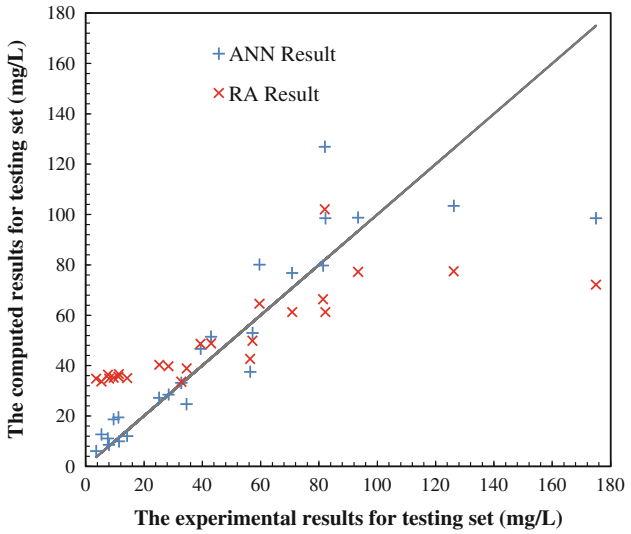

Fig. 5 Comparison of the computed results with the experimental results for testing set

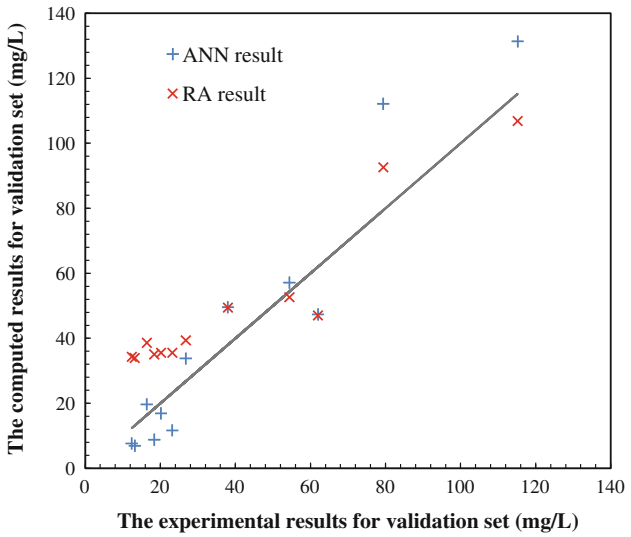

Fig. 6 Comparison of the computed results with the experimental results for validation set

Table 6 The error values for each method

Model no	RMSE (mg/L) for testing		MAE (mg/L) for testing		RMSE (mg/L) for validation		MAE (mg/L) for validation	
	ANNs	RA	ANNs	RA	ANNs	RA	ANNs	RA
1	22.22	30.58	13.87	18.12	9.78	21.04	6.44	12.75
2	21.98	29.96	12.99	21.88	28.83	16.67	25.10	12.25
3	22.71	27.80	14.92	20.04	13.97	28.79	9.82	18.18
4	21.75	26.71	15.18	17.49	16.01	29.89	11.05	19.38
5	21.85	29.91	12.83	22.11	15.02	15.88	10.51	14.65
6	21.09	27.51	11.55	20.25	14.98	16.10	11.01	14.57
7	20.38	29.43	11.67	21.56	13.05	15.35	10.29	14.28

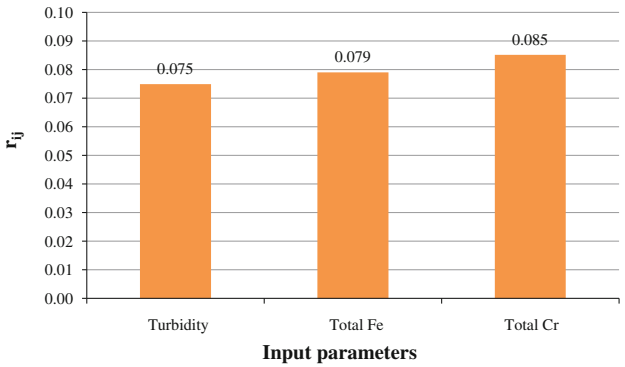

Fig. 7 Sensitivity analysis

sensitivity analysis methods that is used to express similarity relations between the related parameters [15, 35]. In this method, all the relevant data pairs are expressed in a common X-space. The data array X can be defined as:

$$X = \{x_1, x_2, \ldots, x_m\} \tag{10}$$

Each of the elements, x_i, in the data array X is a vector of length m, that is:

$$X_i = \{x_{1m}, x_{2m}, \ldots, x_{im}\} \tag{11}$$

Thus, each of data set is a point in m-dimensional space, where each point requires m-coordinates for a full description. Each point of this space has relation with the final results in a pairwise comparison [16]. The amount of the relation between the data sets, x_i and x_j, is denoted by Eq. (12).

$$r_{ij} = \frac{\sum_{k=1}^{m} x_{ik} x_{jk}}{\sqrt{\sum_{k=1}^{m} x_{ik}^2 \sum_{k=1}^{m} x_{jk}^2}} \tag{12}$$

Figure 7 shows the strengths of relations between output (SSC) and input (turbidity, total Fe, total Cr) parameters. As can be observed in Fig. 7, the most effective parameter on the SSC is total Cr, and then total Fe and turbidity follow.

8 Conclusion

In this study, the ability of the artificial neural networks (ANNs) model to estimate suspended sediment concentration (SSC), for the first time, based on the water quality (WQ) variables, namely total chromium (Cr) concentration, total iron (Fe) concentration, and nephelometric turbidity, was investigated and justified in case of the stream Harsit. The main conclusions that can be drawn in the present study are as follows:

- This study proposes model 7 as a suitable ANN model to efficiently estimate the SSC for the stream Harsit. The purposed ANN model predicted the SSC better than the regression models. The model including all of the independent variables has a root mean square error (RMSE) with 20.38 mg/L and a mean absolute error (MAE) with 11.67 mg/L for testing set.
- Among RA models, model 7 (Eq. 9), which considers all three WQ variables in the input vector, can be suggested as a prediction tool for the SSC.
- Sensitivity analysis revealed that total Cr is a more effective parameter on the SSC than total Fe and turbidity.
- The ANNs model gave satisfactory prediction of the SSC using the WQ variables. This may imply that it can be a useful tool for the prediction of the SSC in Turkish streams and rivers. Therefore, the ANNs model may provide great convenience in water research and for environmental managers.

Acknowledgments This work was supported by the Research Fund of Karadeniz (Black Sea) Technical University, project no. 2007. 118.01.2.

References

1. Williamson TN, Crawford CG (2011) Estimation of suspended sediment concentration from total suspended solids and turbidity data for Kentucky, 1978–1995. J Am Water Resour Assoc 47:739–749
2. Cobaner M, Unal B, Kisi O (2009) Suspended sediment concentration estimation by an adaptive neuro-fuzzy and neural network approaches using hydro-meteorological data. J Hydrol 367:52–61
3. Tayfur G, Guldal V (2006) Artificial neural networks for estimating daily total suspended sediment in natural streams. Nord Hydrol 37:69–79
4. Yang CT (1996) Sediment transport theory and practice. McGraw-Hill, New York
5. EIE (2006) Suspended sediment data for surface waters in Turkey. General Directorate of Electrical Power Resources Survey and Development Administration, Ankara
6. Ulke A, Tayfur G, Ozkul S (2009) Predicting suspended sediment loads and missing data for Gediz River, Turkey. J Hydrol Eng 14:954–965
7. Dogan E, Tripathi S, Lyn DA, Govindaraju RS (2009) From flumes to rivers: can sediment transport in natural alluvial channels be predicted from observations at the laboratory scale. Water Resour Res 45:W08433
8. Dogan E, Yuksel I, Kisi O (2007) Estimation of Total Sediment Load Concentration Obtained by Experimental Study Using Artificial Neural Networks. Environ Fluid Mech 7:271–288
9. Nagy HM, Watanabe K, Hirano M (2002) Prediction of sediment load concentration in rivers using artificial neural network model. J Hydraul Eng ASCE 128:588–595
10. Minella JPG, Merten GH, Reichert JM, Clarke RT (2008) Estimating suspended sediment concentrations from turbidity measurements and the calibration problem. Hydrol Process 22:1819–1830
11. Meral R, Dogan E, Demir Y (2010) Turbidity measurements and modified imhoff cone method for estimation of suspended sediment concentration. Fresenius Environ Bull 19:3066–3072
12. Kang JY, Song JH (1998) Neural network applications in determining the fatigue crack opening load. Int J Fatigue 20:57–69
13. Bayram A, Kankal M, Ozsahin TS, Saka F (2011) Estimation of the carbon to nitrogen ratio in compostable solid waste using artificial neural networks. Fresenius Environ Bull 20:3250–3257
14. Kankal M, Yuksek O (2012) Artificial neural network approach for assessing harbor tranquility: the case of Trabzon Yacht Harbor, Turkey. Appl Ocean Res 38:23–31
15. Majdi A, Rezaei M (2012) Prediction of unconfined compressive strength of rock surrounding a roadway using artificial neural network. Neural Comput Appl. doi:10.1007/s00521-012-0925-2
16. Monjezi M, Mehrdanesh A, Malek A, Khandelwal M (2012) Evaluation of effect of blast design parameters on flyrock using artificial neural networks. Neural Comput Appl. doi:10.1007/s00521-012-0917-2
17. Sengorur B, Dogan E, Koklu R, Samandar A (2006) Dissolved oxygen estimation using artificial neural network for water quality control. Fresenius Environ Bull 15:1064–1067
18. Dogan E, Ates A, Yilmaz EC, Eren B (2008) Application of artificial neural networks to estimate wastewater treatment plant inlet biochemical oxygen demand. Environ Prog 27:439–446
19. Dogan E, Sengorur B, Koklu R (2009) Modeling biological oxygen demand of the Melen River in Turkey using an artificial neural network technique. J Environ Manag 90:1229–1235
20. Kisi O, Yuksel I, Dogan E (2008) Modelling daily suspended sediment of rivers in Turkey using several data-driven techniques. Hydrol Sci J 53:1270–1285
21. Rajaee T, Mirbagheri SA, Zounemat-Kermani M, Nourani V (2009) Daily suspended sediment concentration simulation using ANN and neuro-fuzzy models. Sci Total Environ 407:4916–4927
22. Wang YM, Kerh T, Traore S (2009) Neural networks approaches for modelling river suspended sediment concentration due to tropical storms. Global Nest J 11(457):466
23. Mount NJ, Abrahart RJ (2011) Load or concentration, logged or unlogged? Addressing ten years of uncertainty in neural network suspended sediment prediction. Hydrol Process 25:3144–3157
24. Bayram A, Kankal M, Onsoy H (2012) Estimation of suspended sediment concentration from turbidity measurements using artificial neural networks. Environ Monit Assess 184:4355–4365
25. Demirci M, Baltaci A (2012) Prediction of suspended sediment in river using fuzzy logic and multilinear regression approaches. Neural Comput Appl. doi:10.1007/s00521-012-1280-z
26. Tayfur G (2012) Soft computing in water resources engineering: artificial neural networks, fuzzy logic and genetic algorithms. WIT Press, Southampton
27. Bayram A, Kankal M, Onsoy H, Bulut VN (2010a) The effects of hydraulics structures in the stream Harşit on suspended sediment transport. In: Karahan H, Baykan NO (eds) VI. Ulusal Hidroloji

Kongresi. Denizli, Turkey, pp. 873–882 (in Turkish with English abstract)
28. Bayram A, Onsoy H, Bulut VN, Tufekci M (2010b) Dissolved oxygen levels in the stream Harşit (Turkey). In: 9th International congress on advances in civil engineering, Trabzon, Turkey (full text in CD: ACE2010-HYD-041)
29. Bayram A, Onsoy H, Bulut VN, Tufekci M (2010c) Effect of Torul and Kürtün dams on suspended sediment concentration in the stream Harşit (Turkey). In: 9th International congress on advances in civil engineering, Trabzon, Turkey (full text in CD: ACE2010-HYD-042)
30. Bayram A, Onsoy H, Akinci G, Bulut VN (2011) Variation of total organic carbon content along the stream Harsit, Eastern Black Sea Basin, Turkey. Environ Monit Assess 182:85–95
31. Bayram A, Onsoy H, Komurcu MI, Bulut VN (2012) Effects of Torul dam on water quality in the stream Harsit NE Turkey. Environ Earth Sci 65:713–723
32. Bayram A, Onsoy H, Bulut VN, Akinci G (2012) Influences of urban wastewaters on the stream water quality: a case study from Gumushane Province, Turkey. Environ Monit Assess. doi:10.1007/s10661-012-2632-y
33. Bayram A (2011) A study on seasonal variation of the stream Harsit water quality and estimation of the suspended sediment concentration using artificial neural networks. PhD Thesis, Karadeniz Technical University, Trabzon, Turkey (in Turkish with English abstract)
34. APHA (1992) American Public Health Association. Standard methods for the examination of water and wastewater, 18th edn. Washington
35. Jogn YH, Lee CI (2004) Influence of geological condition on the powder factor for tunnel blasting. Int J Rock Mech Min Sci 41:533–538